



## Pectin/poly(acrylamide-co-acrylamidoglycolic acid) pH sensitive semi-IPN hydrogels: selective removal of $\text{Cu}^{2+}$ and $\text{Ni}^{2+}$ , modeling, and kinetic studies

N. Sivagangi Reddy<sup>a</sup>, K. Madhusudana Rao<sup>b</sup>, T.J. Sudha Vani<sup>a</sup>, K.S.V. Krishna Rao<sup>a,\*</sup>, Yong Ill Lee<sup>c</sup>

<sup>a</sup>Department of Chemistry, Yogi Vemana University, Kadapa 516 003, India, Tel. +91 9440625359; email: [siva0406@gmail.com](mailto:siva0406@gmail.com) (N. Sivagangi Reddy), Tel. +91 9441738560; email: [sudhatiruchuru@gmail.com](mailto:sudhatiruchuru@gmail.com) (T.J. Sudha Vani), Tel. +91 9704278890; emails: [drksvkrishna@yahoo.com](mailto:drksvkrishna@yahoo.com), [ksvkr@yogivemanauniversity.ac.in](mailto:ksvkr@yogivemanauniversity.ac.in) (K.S.V. Krishna Rao)

<sup>b</sup>Department of Polymer Science and Engineering, Pusan National University, Busan, South Korea, Tel. +82 515102407; email: [msraochem@gmail.com](mailto:msraochem@gmail.com)

<sup>c</sup>Department of Chemistry, Changwon National University, Changwon, South Korea, Tel. +82 1027693436; email: [yilee@changwon.ac.kr](mailto:yilee@changwon.ac.kr)

Received 4 November 2014; Accepted 9 January 2015

### ABSTRACT

In this study, we have developed pH sensitive potential semi-IPN hydrogels which are composed from pectin, acrylamide, acrylamidoglycolic acid using *N,N'*-methylene-bis-acrylamide as a cross-linker. The formation and morphology of semi-IPNs were confirmed by FTIR and SEM studies. Swelling and metal ion uptake studies of the semi-IPN hydrogels were performed for  $\text{Cu}^{2+}$  and  $\text{Ni}^{2+}$  ions. Competitive adsorption studies were also carried out for  $\text{Cu}^{2+}$ ,  $\text{Co}^{2+}$ , and  $\text{Ni}^{2+}$ . Further the kinetics data were fitted with pseudo-first and pseudo-second-order kinetic models to investigate the adsorption mechanism. The equilibrium data were interpreted by the Langmuir, Freundlich, and Temkin models. The maximum adsorption capacity of semi-IPN hydrogels calculated from the Langmuir model was found to be 203.7 and 121.7  $\text{mg g}^{-1}$  for  $\text{Cu}^{2+}$  and  $\text{Ni}^{2+}$  ions, respectively. The adsorption process is described by a pseudo-second-order kinetic model.

*Keywords:* Hydrogels; Semi-IPNs; Pectin; Metal ion; Copper; Nickel

### 1. Introduction

Heavy metal pollutants are mainly resulted from many industries, like metal cleaning, mining activities, metal finishing, etc. When these heavy metals are released into the environment, they can cause severe damages to the human body which including accumulating poison, brain damage, and cancer. Therefore, the removal of heavy metal ions from wastewater is

extremely important. During past decade, several methods have been adapted for efficient removal of toxic heavy metals from environments including coagulation, ion exchange treatment, membrane filtration, and electrochemical technologies [1]. But these methods got limited success to achieve high efficiency because they require more time and high cost to separate toxic metals from toxic sludge and other waste products [2–4]. Adsorption process offers potential advantages compared with other methods because of flexibility in design and operation, high-quality treated

\*Corresponding author.

effluent, reversible nature for multiple uses, and many commercially available adsorbent materials, such as activated carbon [5], zeolite [6–9], clay [10,11], sawdust [12], bark [13], biomass [14,15], and natural polymer based adsorbents [16–19]. Recently, among these kinds of conventional adsorbent materials, hydrogel-based adsorbents have attracted growing as they play a crucial role in the removal of heavy metal ions [20–23].

There are a huge number of reports on natural polymers which are used for the separation of metal ions. Cross-linked chitosan/PVA blend beads were developed for the removal of  $\text{Cu}^{2+}$  ions [24,25], orange peel xanthate was used for the removal of  $\text{Cu}^{2+}$  and  $\text{Ni}^{2+}$  ions [26], and also cinnamoyl derivatives of chitosan used for uptake of  $\text{Cu}^{2+}$  and other metal ions [27]. Chitosan-2-aminopyridine glyoxal Schiff's base magnetic nanocomposites were developed for the removal of  $\text{Cu}^{2+}$  and  $\text{Ni}^{2+}$  ions [28]. Recently, pectin-based iron oxide magnetic nanocomposite has been applied for the removal of  $\text{Cu}^{2+}$  ions [29].

Pectin is an anionic plant polysaccharide of D-galacturonic acid linked by  $\alpha(1\rightarrow4)$  glycosidic linkages with variable degree of methylation. Commercial pectin is mainly extracted from apple pomace [30,31] and citrus peels [32,33]. Pectin shows the most favorable association with metal ions called "shifted" egg-box model of metal binding mechanism which is formed between two neighboring chains, stabilized by van der Waals interactions and hydrogen bonds in addition to electrostatic interactions [34,35]. Semi-interpenetrating polymer networks (semi-IPNs) are a class IPNs which can be prepared with multifunctionality to yield required properties. Hence, the semi-IPNs exhibit response in both pH and temperature. pH sensitive properties of hydrogels are important in fields drug delivery systems [36,37], sanitary adsorbent materials, metal ion removal [38] applications. Pulsatile and on-off switching pH-sensitive behavior can be observed by both  $-\text{COOH}$  and  $-\text{NH}_2$  groups present in the in case of low pH medium 1–5 amines groups are ionized to  $-\text{NH}_3^+$ , where as in high-pH medium 8–14 acid groups are ionized to  $-\text{COO}^-$  and cause structural changes to the hydrogels by ionic interactions.

Recently, we have developed thiourea-formaldehyde cross-linked chitosan membrane networks and polyaniline-co-poly(acrylic acid) grafted sodium alginate/gelatin membranes for the separation of  $\text{Cu}^{2+}$  and  $\text{Ni}^{2+}$  ions [16,17]. Poly(acrylamidoglycolic acid) (PAGA) contains  $-\text{OH}$ ,  $-\text{COOH}$ , and  $-\text{CONH}-$  functional groups that show excellent selectivity toward the separation of bivalent metal ions [39,40]. This chelation behavior of PAGA led us to explore its usefulness for developing a new semi-IPN. In continuation of our research, we are now developed pectin-based semi-IPN

for the removal of  $\text{Cu}^{2+}$  and  $\text{Ni}^{2+}$  ions. The developed semi-IPN system is designed with natural (pectin) and synthetic polymer (PAGA), which enhances the anionic, hydrophilic as well as chelation behavior. The effect of pH, temperature, monomer concentration, and initial metal ion concentration were investigated. In order to better understand the adsorption characteristics, kinetic models like pseudo-first-order and pseudo-second order were worked out. Isotherm models like Langmuir, Freundlich, and Temkin were employed to evaluate the sorption process.

## 2. Experimental

### 2.1. Materials

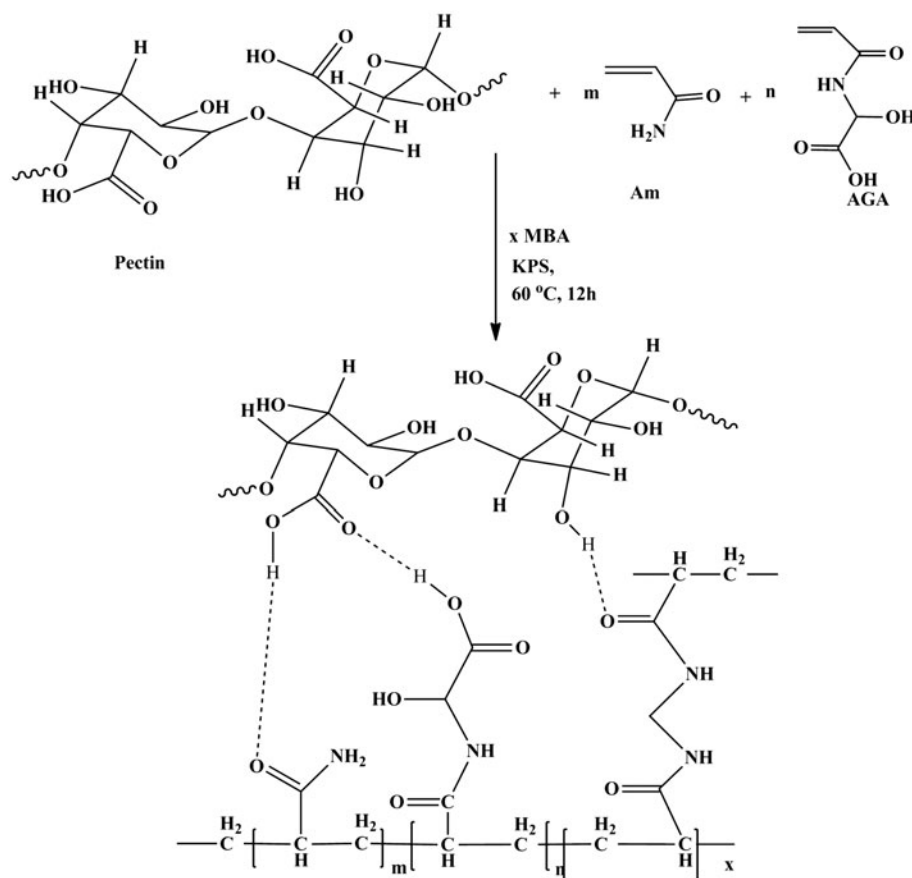
Synthetic grade acrylamidoglycolic acid (AGA) is purchased from Sigma-Aldrich (St. Louis, MO, USA). Synthetic grade pectin, potassium persulfate (KPS), and acrylamide (Am) were purchased from Merck (Mumbai, India). Analytical grade cupric nitrate is obtained from Qualigens (Mumbai, India). Synthetic grade reagents of *N,N'*-methylene-bis-acrylamide (MBA), nickel ammonium sulfate, and analytical grade cobaltous chloride were purchased from S.D Fine chemicals (Mumbai, India). Throughout the whole experiment, double-distilled water was used.

### 2.2. Preparation of pectin-based semi-IPN hydrogels

Pectin/poly(Am-co-AGA-cl-MBA) (PPAA) semi-IPN hydrogels were prepared by a free radical polymerization and the composition of semi-IPN hydrogels is given in Table 1. The persulfate initiator is reduced to the anion radical  $[(\text{SO}_4)^{\cdot-}]$ , these anion radical extracts hydrogen from the AGA, Am, and cross-linker MBA to form respective vinyl radicals and initiate the copolymerization to produce pectin/poly(Am-co-AGA-cl-MBA) hydrogels, pectin as guest polymer. The structure of prepared PPAA hydrogels is given in Fig. 1.

Table 1  
Composition of monomers in PPAA semi-IPN hydrogels

Formulation	Am (g)	AGA (g)	Pectin (mL)	MBA (1%) (mL)	KPS (5%) (mL)
A	0.5	0.125	2	1.0	1
B	0.5	0.25	2	1.0	1
C	0.5	0.50	2	1.0	1
D	0.5	0.25	2	2.0	1
E	0.5	0.25	2	0.5	1
F	0.5	0.00	2	1.0	1



Schematic representation of PPAA semi-IPN hydrogels

Fig. 1. Schematic representation of PPAA semi-IPN hydrogels.

Monomers, Am and AGA were dissolved in 3 mL of distilled water and then 2 mL of pectin solution (2 wt.%), 1.0 mL of cross-linking agent MBA (1 wt.%) aqueous solution and 1.0 mL of KPS (5 wt.% aqueous solution) were added. The resulting solution was kept at 60 °C for 12 h to complete the formation of semi-IPN hydrogels. The formed hydrogels were kept in double-distilled water for about a week by frequently changing the water in order to remove the unreacted monomers and KPS. Then, the gels were dried in vacuum oven at 50 °C.

### 2.3. Swelling studies

The swelling characteristics of the PPAA semi-IPN hydrogels were studied by the following method described. The hydrogel samples were dried to obtain xerogels which were used for swelling studies. The xerogels were weighed and then immersed in a 500 mL glass beaker containing double-distilled water

at 25 °C. At specific intervals of time, the weight of swollen hydrogels was taken by removing the excess water on the surface of the gels. The operation was repeated until no significant change of weights was detected and swelling ratio ( $Q_s$ ) was calculated by following equation:

$$Q_s = \frac{W_s - W_d}{W_d} \quad (1)$$

where  $W_s$  is the weight of the swollen PPAA semi-IPN hydrogel and  $W_d$  is the weight of the dried PPAA semi-IPN hydrogel. The equilibrium swelling studies also done with different pH solutions varying from 2 to 10.

### 2.4. Adsorption studies

The adsorption studies of  $\text{Cu}^{2+}$  and  $\text{Ni}^{2+}$  ions on PPAA semi-IPN hydrogels were carried out by batch

experimental studies. PPAA semi-IPN hydrogels were added to the test solutions and kept for equilibrium. Finally, the resulted solution was used to determine its metal content by atomic absorption spectrometry (AAS) (GBC, Avanta, Australia). All the data reported in this study are based on the average of three replicate measurements on each sample solution for sorption and desorption studies.

### 2.5. Characterization

Fourier transform infrared spectroscopy (FTIR) measurements were performed with pure pectin, PPAA semi-IPN hydrogels, and metal sorbed PPAA semi-IPN hydrogels using PerkinElmer FTIR spectrometer (Beaconsfield, UK). The sample pellets were prepared by grinding PPAA semi-IPN hydrogels finely with KBr and pressing them under the hydraulic pressure of 600 dynes/m<sup>2</sup>. The spectra were obtained between 4,000 and 500 cm<sup>-1</sup>. Scanning electron microscope (SEM) images of the PPAA semi-IPN hydrogels were recorded using a SEM (ZEISS EVO MA15, Oxford Instrument, UK) at the required magnifications.

## 3. Results and discussion

### 3.1. FTIR spectroscopy

FTIR spectra of pure pectin, PPAA semi-IPN hydrogels, and metal ions (Cu<sup>2+</sup> and Ni<sup>2+</sup>)-loaded PPAA hydrogels are shown in Fig. 2. The FTIR spectrum of PPAA semi-IPN hydrogel shows a strong amide-I band at 1,656 cm<sup>-1</sup> which is the characteristic

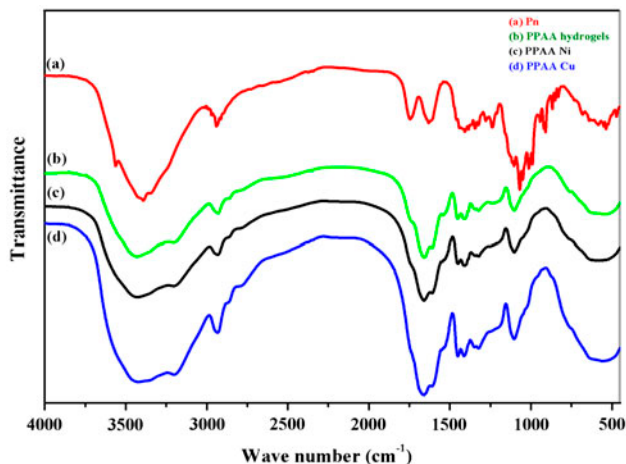


Fig. 2. FTIR spectra of pure pectin, PPAA semi-IPN hydrogels, and metal ions (Cu<sup>2+</sup> and Ni<sup>2+</sup>)-loaded PPAA hydrogels.

of the C=O stretching vibrations of the amide group. A strong characteristic amide-II band which arises from the couplings of in-plane N–H bending and C–N stretching vibrations of the C–N–H group is observed at 1,542 cm<sup>-1</sup>. These two bands (amide-I and II) are the characteristics for amides because of their constant position and strong intensities [41,42]. A broad and merged band at 3,000–3,400 cm<sup>-1</sup> belongs to both –OH and –NH stretching. It can be thought that poly(Am-co-AGA-cl-MBA) is the host polymer and pectin is guest in this semi-IPN system. Intermolecular forces between the pectin and host in semi-IPN hydrogels are also shown in Fig. 1 [38,43].

In case of Cu<sup>2+</sup> loaded hydrogels, the intensities of all peaks become higher than pristine PPAA hydrogels and also the peak maximum of amide band is shifted from 1,656 to 1,662 cm<sup>-1</sup>, peak at 1,407 cm<sup>-1</sup> is shifted to 1,413 cm<sup>-1</sup>. This may be due to large amount of Cu<sup>2+</sup> present in the PPAA semi-IPN hydrogels. Where as in case of Ni<sup>2+</sup> loaded hydrogels, there is little increase in the intensity of 1,407 cm<sup>-1</sup> peak. This may be due to less amount of Ni<sup>2+</sup> in the PPAA semi-IPN hydrogels. This shows that this semi-IPN hydrogels have higher adsorption capacity for Cu<sup>2+</sup> ions than the Ni<sup>2+</sup> ions.

### 3.2. Scanning electron microscopy

SEM images of the single PPAA semi-IPN hydrogel taken at 5.0 and 10 k $\times$  magnifications are shown in Fig. 3. It was found that smooth surface was formed, possibly due to the formation of the mixture of linear and cross-linked polymer chains in the hydrogel.

### 3.3. Swelling studies

Swelling kinetics data of PPAA semi-IPN hydrogels are shown in Fig. 4. From figure shows that the maximum swelling is obtained at 1950 min, the maximum swelling ratio of different formulations (shown in Table 1) of PPAA semi-IPN hydrogels were 30, 35, 67, 19, 41, and 12 in distilled water. Swelling ratio of PPAA semi-IPN hydrogels in water is maximum for formulation C and minimum for formulation F. The water uptake capacity of PPAA semi-IPN hydrogel increases with the decrease in amount of cross-linking agent and increase in AGA amount. Increasing in swelling ratio may be due to increase in the hydrophilic character of semi-IPN hydrogels as increase in the hydroxyl and carboxylic acid groups of PAGA. Equilibrium swelling ratios of the hydrogels at different pH (2–10) solutions were determined and shown in Fig. 5. When pH is increased from 2 to 10, equilibrium swelling of hydrogels is increased due to

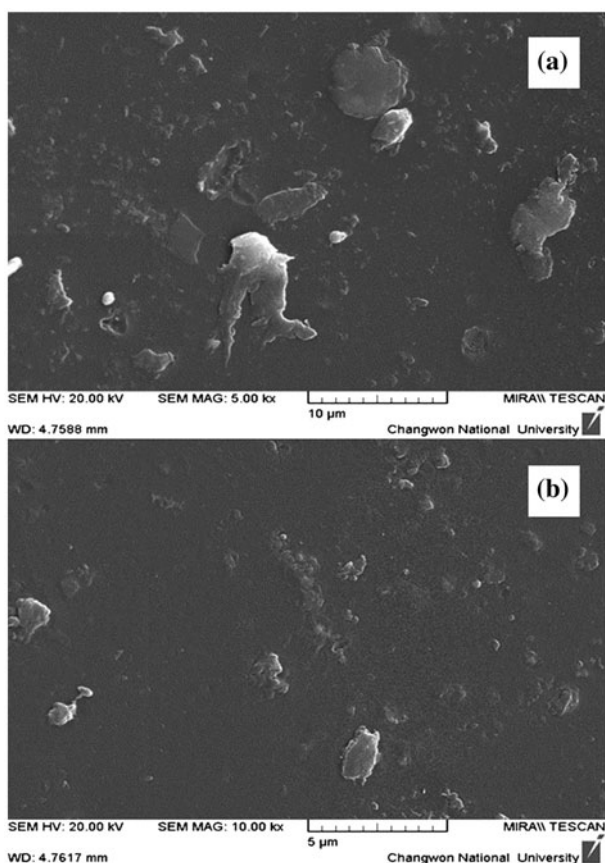


Fig. 3. SEM images of formulation C of PPAA semi-IPN hydrogels with 5 and 10× magnifications.

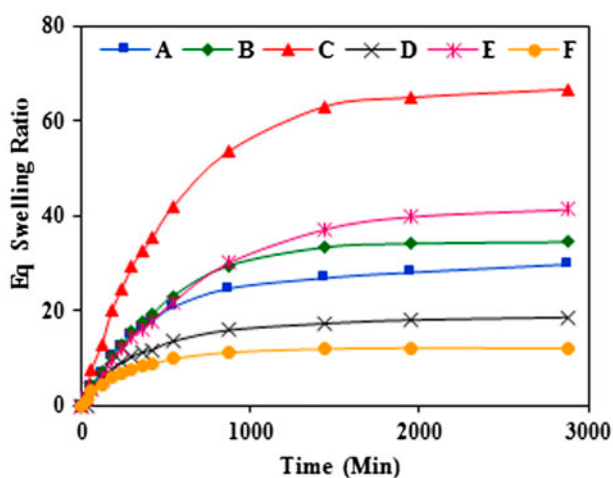


Fig. 4. Swelling kinetics of PPAA semi-IPN hydrogels A–F.

electronic repulsion of  $\text{COO}^-$  ions produced from  $-\text{COOH}$  group [44]. The trend of increase in equilibrium swelling ratio is similar to increase in the

ratio of AGA monomer and cross-linking ratio in the hydrogels.

### 3.4. Static adsorption studies

The sorption studies of the  $\text{Cu}^{2+}$  and  $\text{Ni}^{2+}$  ions on the PPAA semi-IPN hydrogels were carried out by batch experiments studies. To the test solutions, added PPAA semi-IPN hydrogels and kept for equilibrium time. Finally, the resulted solution was used for determining its metal ion content by AAS.

To the test solutions prepared in the range 1–6 mM for concentration effect and 4 mM for remaining studies, added about 50 mg of PPAA semi-IPN hydrogels and kept for equilibrium adsorption using a thermostat to attain equilibrium. The metal concentrations before and after the adsorption were measured using AAS. The metal concentrations before and after the adsorption ( $C_o$  and  $C_e$ , respectively) and the dry weight of the adsorption gel ( $W$ ), as well as the volume of aqueous solution ( $V$ ), the amount of adsorption ( $Q_e$ ) were calculated using an Eq. (2).

$$Q_e = \frac{C_o - C_e}{W} \times V \quad (2)$$

### 3.5. Effect of pH

The effect of pH on adsorption capacity was conducted by mixing 0.05 gm PPAA adsorbents with 30 mL of 4 mM  $\text{Cu}^{2+}$  and  $\text{Ni}^{2+}$  ions in aqueous solution with different pH value ranging from 1 to 5 static condition for 24 h on water bath, then the residual metal concentrations were determined. The effect of pH on adsorption capacity is shown in Fig. 6.

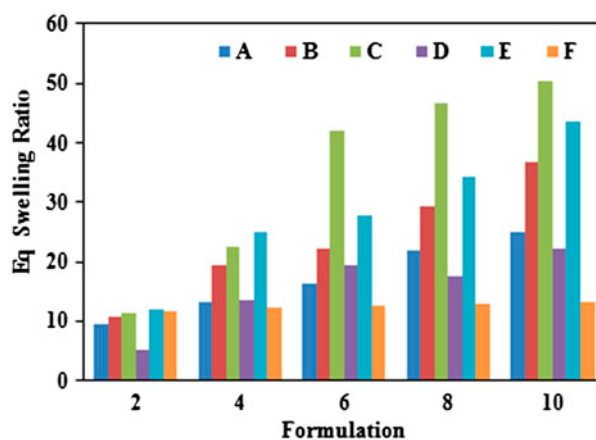


Fig. 5. Effect of pH on equilibrium swelling of PPAA semi-IPN hydrogels A–F.

As the pectin is pH responsive, when pH is increased the adsorption also increased. Although the maximum is at pH 7, we stopped at pH 5, because of the precipitation of  $\text{Cu}^{2+}$  and  $\text{Ni}^{2+}$  ions at higher parts of the concentration range [45,46].

### 3.6. Effect of monomer

To investigate the effect of adsorbent dosage on the adsorption capacity, 30 mL of 4 mM  $\text{Cu}^{2+}$  and  $\text{Ni}^{2+}$  solutions was adjusted to pH 5, followed by addition of various amount of PPAA semi-IPN hydrogels. After equilibrium time, the residual metal concentrations were analyzed. The effect of monomer on adsorption capacity is shown in Fig. 7. As the formulation F doesn't have AGA it indicates minimum adsorption. As the monomer concentration is increased the adsorption is increased for formulations A–C, and further increase at formulation D is due to increase in the cross-linking agent which causes polymer chains to be close enough for easy binding of metal ions by chelation. Decrease in adsorption at formulation E is due to decrease in the amount of cross-linking agent, and decrease in formulation F is due to the absence of AGA monomer.

### 3.7. Adsorption kinetics

The influence of the contact time on the adsorption was investigated for PPAA semi-IPN hydrogels. The experiment was carried out with concentration of 30 mL of 4 mM  $\text{Cu}^{2+}$  and  $\text{Ni}^{2+}$  at pH 5. The adsorption equilibrium conditions were reached after about 12 h for  $\text{Ni}^{2+}$  and 24 h, minimum time to take adsorption

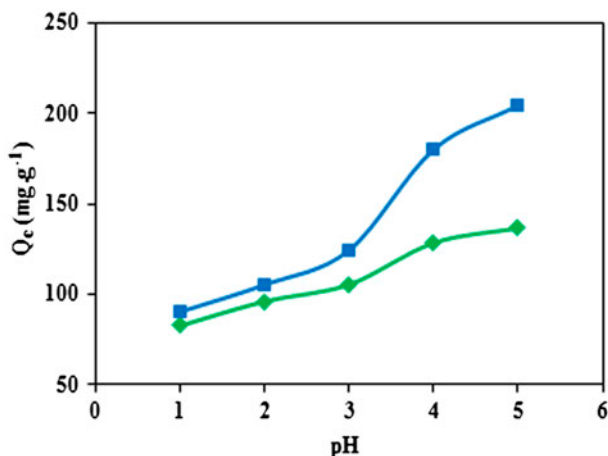


Fig. 6. Effect of pH for adsorption of  $\text{Cu}^{2+}$  (■) and  $\text{Ni}^{2+}$  (◆) ions on PPAA semi-IPN hydrogels.

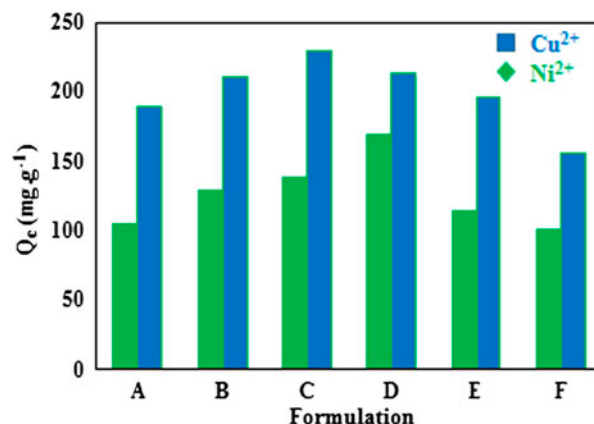


Fig. 7. Effect of monomer for adsorption of  $\text{Cu}^{2+}$  (■) and  $\text{Ni}^{2+}$  (◆) ions on PPAA semi-IPN hydrogels.

equilibrium and it is decided by constant adsorption with time in the graph  $Q_e$  vs. time. The effect of contact time on equilibrium adsorption is shown in Fig. 8. Adsorption dynamics is used to describe the solute uptake rate which controls the residence time of adsorbate uptake at the solid–solution interface. Two kinetics models were used to analyze adsorption kinetics, namely, pseudo-first order and pseudo-second order. The pseudo-first-order model is presented by the following equation:

$$\log(C_e - Q_t) = \log C_e - \frac{K_1}{2.303} t \quad (3)$$

The plot of  $\log(C_e - Q_t)$  against  $t$  provides a linear relationship from which  $K_1$ , constant of pseudo-first-order adsorption ( $\text{min}^{-1}$ ) using  $Q_t$  is the adsorption capacity at time  $t$ , ( $\text{mg g}^{-1}$ ) and  $C_e$ . The pseudo-second-order model is presented by the following equation:

$$\frac{t}{Q_t} = \frac{1}{K_2 Q_e^2} + \frac{t}{Q_e} \quad (4)$$

The plot of  $t/Q_t$  against  $t$  provides a linear relationship from which  $K_2$ , rate constant of pseudo-second-order adsorption ( $\text{g mg}^{-1} \text{min}^{-1}$ ) and  $Q_e$ , adsorption capacity at equilibrium ( $\text{mg g}^{-1}$ ) are determined from the slope and intercept of the curve.

The kinetic parameters for adsorption of  $\text{Cu}^{2+}$  and  $\text{Ni}^{2+}$  ions by PPAA semi-IPN hydrogels are given in Table 2 and graphs are shown in Fig. 8. The experimental  $Q_e$  values are in agreement with the calculated values using pseudo-first-order and

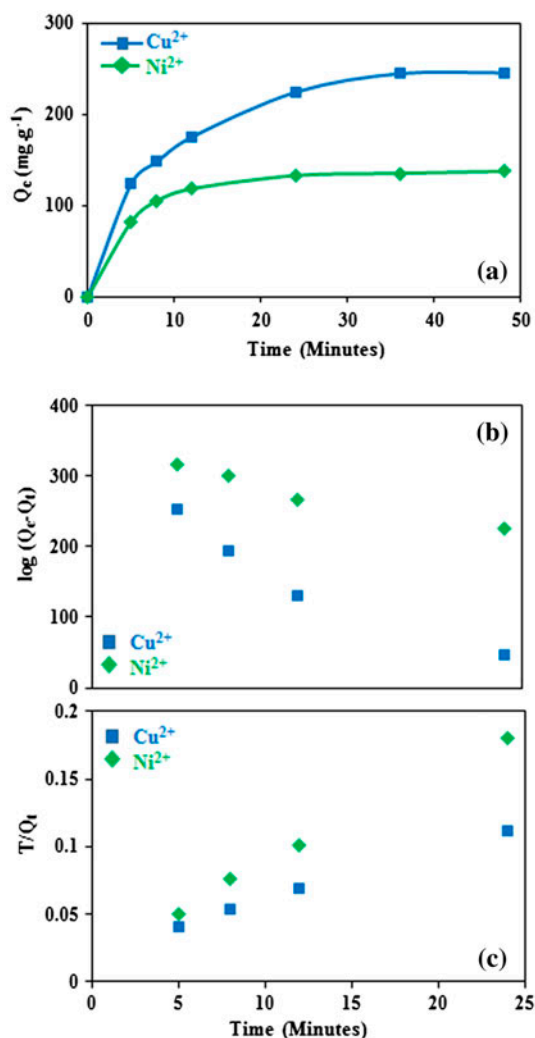


Fig. 8. Effect of (a) contact time (b) first order (c) second order for adsorption of Cu<sup>2+</sup> (■) and Ni<sup>2+</sup> (◆) ions on PPAA semi-IPN hydrogels.

pseudo-second-order kinetics. Based on the obtained correlation coefficients ( $r^2$ ), the pseudo-second-order equation was the model that furthered the best fit for the experimental kinetic data, suggesting chemical sorption as the rate-limiting step of the adsorption mechanism and no involvement of a mass transfer in solution [47].

### 3.8. Adsorption isotherms

The sequential adsorption data of single-metal ion species are useful to investigate the metal ion adsorption performances in single-metal ion system. The metal ion adsorption data from the isotherm adsorption experiments can be fitted with Langmuir, Freundlich, and Temkin models that provide useful

Table 2

Kinetic models and constants for adsorption of Cu<sup>2+</sup> and Ni<sup>2+</sup> ions by PPAA semi-IPN hydrogels

Metal ions	$K_t (b) \times 10^{-2}$	$Q_{et}$	$r^2$
<i>First order model</i>			
Cu <sup>2+</sup>	12.7	0.243	0.980
Ni <sup>2+</sup>	16.8	0.297	0.966
<i>Second order model</i>			
Cu <sup>2+</sup>	45.1	1.848	0.999
Ni <sup>2+</sup>	152.8	2.681	0.997

information such as the maximum adsorption capacity, adsorption affinity, and heat of adsorption [48–50].

The isotherms were linearized by several batch experiments, PPAA semi-IPN hydrogels were equilibrated with varying initial concentrations of Cu<sup>2+</sup> and Ni<sup>2+</sup> ions at pH 5.0. Although optimum pH was found as 7.0, the adsorption capacity of Cu<sup>2+</sup> and Ni<sup>2+</sup> ions on the PPAA semi-IPN hydrogels was studied at pH 5.0, because of the precipitation of Cu<sup>2+</sup> and Ni<sup>2+</sup> ions at higher parts of the concentration range. After equilibrium time, the hydrogels were removed from the solutions and the solutions were analyzed by AAS for residual amount of metal ions.

All the Langmuir, Freundlich, and Temkin models of the single species metal ion isotherm adsorption fitting parameters are given in Table 3.

Langmuir isotherm is given by the Eq. (5). where  $Q$  is the amount of adsorbed Cu<sup>2+</sup> and Ni<sup>2+</sup> ions on

Table 3

Different isotherm models and constants for adsorption of Cu<sup>2+</sup> and Ni<sup>2+</sup> by PPAA semi-IPN hydrogels

Langmuir isotherm constants			
Metal	$K_L$	$Q_{max}(mg\ g^{-1})$	$r^2$
Cu <sup>2+</sup>	652.80	203.7	0.986
Ni <sup>2+</sup>	0.13	121.7	0.989
Freundlich isotherm constants			
Metal	$K_F$	$N$	$r^2$
Cu <sup>2+</sup>	-0.377	3.28	0.950
Ni <sup>2+</sup>	0.322	0.19	0.975
Temkin isotherm constants			
Metal	$\ln A$	$B$	$r^2$
Cu <sup>2+</sup>	1.548	1,625	0.965
Ni <sup>2+</sup>	0.114	22,109	0.996

the pectin-based hydrogels at equilibrium ( $\text{mol g}^{-1}$ ),  $C_e$  is the equilibrium concentration of  $\text{Cu}^{2+}$  and  $\text{Ni}^{2+}$  ions in solution ( $\text{gm L}^{-1}$ ), and  $Q_{\text{max}}$  and  $b$  are Langmuir constants related to the maximum adsorption capacity and energy of adsorption, respectively. The Langmuir equation can be linearized as Eq. (6) for the determination of Langmuir constants.

$$Q = \frac{Q_{\text{max}} b C_e}{1 + b C_e} \quad (5)$$

$$\frac{C_e}{Q} = \frac{1}{Q_{\text{max}}} C_e + \frac{1}{b Q_{\text{max}}} \quad (6)$$

The Freundlich isotherm model is based on the assumption of adsorption on heterogeneous surfaces and situations that involve multilayer adsorption. The Freundlich isotherm is usually given as below.

$$Q = K_F C_e^{1/n} \quad (7)$$

where  $K_F$  and  $n$  are the Freundlich constants related to adsorption affinity and adsorption intensity, respectively. The Freundlich equation can be linearized in logarithmic form for the determination of Freundlich constants as:

$$\log Q = \frac{1}{n} \log C_e + \log K_F \quad (8)$$

The Temkin isotherm assumes that heat of adsorption (function of temperature) of all molecules in the layer would decrease linearly with coverage [51] as implied in the equation; its derivation is characterized by a uniform distribution of binding energies.

$$Q_e = \frac{RT}{b} \ln A + \frac{RT}{b} \ln C_e \quad (9)$$

It can be found from Table 3 that the model generally fits the Langmuir model isotherm adsorption data better than the Freundlich adsorption, whose results give a higher  $r^2$  values for the Langmuir model fitting than the Freundlich model fitting. The adsorption affinity values of  $K_F$  follow the sequence of  $\text{Ni}^{2+} > \text{Cu}^{2+}$  ions. However, the  $Q_{\text{max}}$  values follow a different trend of  $\text{Cu}^{2+} \gg \text{Ni}^{2+}$ .

### 3.9. Selectivity experiments

The competitive absorption experiments were conducted by preparing mixture of  $\text{Cu}^{2+}$ ,  $\text{Co}^{2+}$ , and  $\text{Ni}^{2+}$  ions, and each metal ion initial concentration was

200  $\text{mg L}^{-1}$  (200 ppm) and the results are shown in Table 4. In order to investigate the selectivity of the adsorbent, static adsorption experiment results were used for evaluation. The selectivity coefficient for the binding of  $\text{Ni}^{2+}$  ions in the presence of competitor ions can be obtained from equilibrium binding data according to the following equation:

$$K = \frac{K_d(\text{Ni}_{\text{II}})}{K_d(\text{M}_{\text{II}})} \quad (10)$$

where  $K$  is the selectivity coefficient,  $K_d$  is the distribution coefficient, and  $(\text{M}_{\text{II}})$  represents  $\text{Co}^{2+}$  and  $\text{Cu}^{2+}$ .  $K$  represents  $\text{Ni}^{2+}$  adsorption selectivity when there are other metal ions in aqueous solution. The larger  $K$  indicates that the system has stronger ability for  $\text{Ni}^{2+}$  ion, same was also expected by larger free energy  $\Delta G^\circ$  values.

### 3.10. Thermodynamic studies

Thermodynamic parameters of adsorption can evaluate the orientation and feasibility of the physico-chemical adsorptive reaction and can provide strong information regarding the inherent energy and structural changes due to metal ion adsorption process. These aspects were determined from the experimental data obtained using the following equations:

$$\ln K_C = -\frac{\Delta H^\circ}{RT} + \frac{\Delta S^\circ}{R} \quad (11)$$

$$\Delta G^\circ = -RT \ln K_C \quad (12)$$

where  $K_C$  is the equilibrium coefficient for the adsorption.  $\Delta S^\circ$ ,  $\Delta H^\circ$ , and  $\Delta G^\circ$  are the change of entropy, enthalpy, and Gibbs free energy,  $T$  is the absolute temperature and  $R$  is gas constant. The values  $\Delta H^\circ$  and  $\Delta S^\circ$  were calculated from the slope and intercept of the Van't Hoff linear plots of  $\ln K_C$  vs.  $1/T$  the results are presented in Table 5 and graph is shown in Fig. 9. The negative value for the Gibbs free energy for

Table 4  
Selectivity studies for  $\text{Cu}^{2+}$ ,  $\text{Ni}^{2+}$ , and  $\text{Co}^{2+}$  ions by PPAA semi-IPN hydrogels

Metal	$C_e$ (ppm)	$C_p$ (ppm)	$K_d$	$K$
Ni	7.70	192.30	24.97	8.00
Co	95.85	104.15	1.09	0.04
Cu	65.90	134.10	2.04	0.08

Table 5

$\Delta G^\circ$  and  $\Delta S^\circ$  of  $\text{Cu}^{2+}$  and  $\text{Ni}^{2+}$  ions adsorption by PPAA semi-IPN hydrogels calculated by Eqs. (11)–(12) at different temperatures

Metal	$1/T \times 10^{-5}$	$C_{\text{equ}}$	$C_{\text{ads}}$	$K_C$	$\ln K_C$	$\Delta G^\circ$	$\Delta H^\circ$	$\Delta S^\circ$
$\text{Cu}^{2+}$	341	53.28	200.92	3.77	1.33	−3.29	–	9.13
	329	53.60	200.60	3.74	1.32	−3.38	554.44	–
	319	53.89	200.30	3.71	1.31	−3.47	–	–
$\text{Ni}^{2+}$	341	24.87	209.88	8.43	2.13	−5.28	1.02	21.17
	329	24.68	210.08	8.51	2.14	−5.48	–	–
	319	24.28	210.47	8.67	2.16	−5.70	–	–

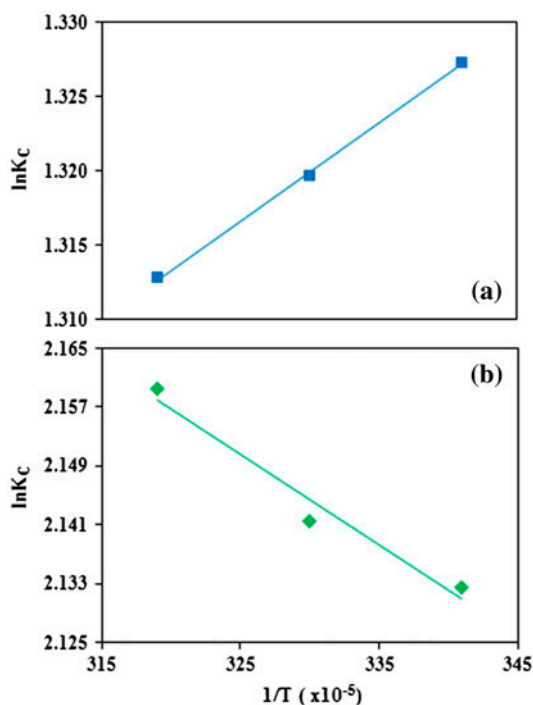


Fig. 9. Temperature effect on adsorption of (a)  $\text{Cu}^{2+}$  (■) and  $\text{Ni}^{2+}$  (◆) ions for PPAA semi-IPN hydrogels.

adsorption of  $\text{Cu}^{2+}$  and  $\text{Ni}^{2+}$  ions shows that the adsorption process is spontaneous and also the degree of spontaneity increases with increasing temperature. The overall adsorption process seems to be exothermic ( $\Delta H^\circ = -5.54 \text{ J mol}^{-1}$ ) for  $\text{Cu}^{2+}$  and endothermic ( $\Delta H^\circ = 10.2 \text{ J mol}^{-1}$ ) for  $\text{Ni}^{2+}$ . Although not very high, these values of  $\Delta H^\circ$  can be interpreted on the basis of considerably strong interaction between metal ions and PPAA semi-IPN hydrogel. One possible explanation of positive  $\Delta H^\circ$  is that the  $\text{Ni}^{2+}$  ions are well solvated, in order to adsorption of the  $\text{Ni}^{2+}$  ions they have to lose part of their hydration sheath, which requires energy that means it is an endothermic process. This energy of dehydration supersedes the

exothermicity of the  $\text{Ni}^{2+}$  ions getting adsorbed to the hydrogel [52]. Entropy has been defined as the degree of  $\Delta S^\circ$  reflects good affinity of the system. The positive values of  $S$  reflect good affinity of metal ions towards PPAA semi-IPN hydrogels, and increased randomness at the solid–solution interface during adsorption of metal ions on to PPAA semi-IPN hydrogels. Since adsorbed metal ions decreases, the number of water molecules increases [53,54]. Moreover, it is found that  $\Delta H < T\Delta S$ , indicating that the influence of  $T\Delta S$  is more remarkable than enthalpy of adsorption. Adsorption is thus likely to occur spontaneously at normal and high temperatures because  $\Delta H - T\Delta S$  is  $< 0$ .

### 3.11. Desorption and reuse studies

Desorption of  $\text{Cu}^{2+}$  and  $\text{Ni}^{2+}$  from gels was studied with HCl and EDTA as regenerants. 0.1 M of HCl and EDTA are used 81 and 92% of desorption was achieved. In case of acid, regenerant protonation of amines and carboxyl groups takes place and metal ions were desorbed in to the solution, whereas affinity of chelation of  $\text{Cu}^{2+}$  and  $\text{Ni}^{2+}$  with EDTA to form EDTA complex is driving force for desorption when we use EDTA as regenerant. The desorbed hydrogels were washed with 0.01 M molar NaOH solution for regeneration of acidic sites for further extraction. The cycle of extraction recovery and regeneration was repeated for five times. The uptake performance of regenerated sorbent was found to be close to the freshly prepared sorbents which indicate that the sorbents can be regenerated and reused, respectively, at least for five times.

### 3.12. Comparison with literature

The adsorption capacity of present work is compared with the literature and is presented in Table 6. It was reported in the literature that Chitosan/PVA beads shows an adsorption capacity of  $47.85 \text{ mg g}^{-1}$  of

Table 6  
Comparison table of present work with literature

S.No	Polymer material	Metal (Cu <sup>2+</sup> /Ni <sup>2+</sup> )	pH	Metal uptake mg g <sup>-1</sup>	Refs.
1	Chitosan/PVA beads	Cu <sup>2+</sup>	–	47.85	[24]
2	Chitosan and cross-linked chitosan beads	Cu <sup>2+</sup>	6.0	80.71	[25]
3	Orange peel xanthate	Cu <sup>2+</sup> /Ni <sup>2+</sup>	–	77.6/15.5	[26]
4	Chitosan derivatives	Cu <sup>2+</sup> /Ni <sup>2+</sup>	5.6	29.3–36.4, 2.4–3.1	[27]
5	Magnetic chitosan-2-aminopyridine glyoxal Schiff's base resin	Cu <sup>2+</sup> /Ni <sup>2+</sup>	5.0	124/67	[28]
6	Pectin based composites	Cu <sup>2+</sup>	5.0	48.99	[29]
7	Pectin/poly (AM-co-AGA)(PPAA) semi-IPN hydrogels	Cu <sup>2+</sup> /Ni <sup>2+</sup>	5.0	203.7/121.7	Present study

Cu<sup>2+</sup> [24]. Chitosan and cross-linked chitosan beads exhibit an adsorption capacity of 80.71 mg g<sup>-1</sup> of Cu<sup>2+</sup> [25]. Orange peel xanthate exhibits an adsorption capacity of 77.6 and 15.5 mg g<sup>-1</sup> for Cu<sup>2+</sup> and Ni<sup>2+</sup>, respectively [26]. Chitosan derivatives exhibit an adsorption capacity of 36.4 and 3.1 mg g<sup>-1</sup> for Cu<sup>2+</sup> and Ni<sup>2+</sup>, respectively [27]. Magnetic chitosan-2-aminopyridine glyoxal Schiff's base resin shows an adsorption capacity of 124 and 67 mg g<sup>-1</sup> for Cu<sup>2+</sup> and Ni<sup>2+</sup>, respectively [28], and pectin-based composites show an adsorption capacity of 48.99 mg g<sup>-1</sup> for Cu<sup>2+</sup> [29]. The adsorption capacity values reported in the present study are higher than the above values reported in the literature. The higher adsorption capacity of PPAA semi-IPN hydrogels is due to the presence of multi-functional groups, such as such as –OH, –COOH and –CONH<sub>2</sub>, which are having better chelation with the metal ions. From this observation, it may be concluded that the PPAA semi-IPN hydrogels have good adsorption capacity for Cu<sup>2+</sup> and Ni<sup>2+</sup> ions.

#### 4. Conclusion

The present study focuses on the synthesis of new PPAA semi-IPN hydrogels, and their characterization by FTIR, SEM, and finally the removal studies of Cu<sup>2+</sup> and Ni<sup>2+</sup> ions from aqueous solution. Adsorption of Cu<sup>2+</sup> and Ni<sup>2+</sup> is depending on pH of the medium and it is found to be effective at pH 5. Equilibrium data were fitted to different isotherm models. Among these models, Langmuir model is in good agreement with the experimental data with high *r*<sup>2</sup> values. Maximum adsorption capacity for Cu<sup>2+</sup> and Ni<sup>2+</sup> ions is 203.7 and 121 mg g<sup>-1</sup>, respectively. Kinetic study showed that the pseudo-second-order model is appropriate to describe the adsorption process. Selectivity studies show that Ni<sup>2+</sup> has more selective than Cu<sup>2+</sup> ion. The dependence of adsorption of Cu<sup>2+</sup> and Ni<sup>2+</sup> ions on temperature was investigated and the

thermodynamic parameters  $\Delta G^\circ$ ,  $\Delta H^\circ$ , and  $\Delta S^\circ$  were calculated. The results showed that adsorption process is feasible, spontaneous, and exothermic. The mechanism of adsorption includes mainly ionic interactions (chemical interactions) between metal cations and PPAA semi-IPN hydrogels. The adsorption–desorption cycle results demonstrated that the regeneration and subsequent use of the PPAA semi-IPN hydrogels would enhance the economics of practical applications for the removal of Cu<sup>2+</sup> and Ni<sup>2+</sup> ions from water and wastewater.

#### Acknowledgments

Authors Dr KSV Krishna Rao and N Siva Gangi Reddy highly thankful to the Board of Research on Nuclear Science, Mumbai, India. (B.R.N.S file No 2010/35C/53/BRNS/2538) for financial support.

#### References

- [1] S. Babel, T.A. Kurniawan, Low-cost adsorbents for heavy metals uptake from contaminated water: A review, *J. Hazard. Mater.* 97(1–3) (2003) 219–243.
- [2] A.J. Pedersen, Characterization and electrolytic treatment of wood combustion fly ash for the removal of cadmium, *Biomass Bioenergy* 25(4) (2003) 447–458.
- [3] G. Borbely, E. Nagy, Removal of zinc and nickel ions by complexation membrane filtration process from industrial wastewater, *Desalination* 240(1–3) (2009) 218–226.
- [4] D. Feng, C. Aldrich, H. Tan, Treatment of acid mine water by use of heavy metal precipitation and ion exchange, *Miner. Eng.* 13(6) (2000) 623–642.
- [5] V.C. Srivastava, I.D. Mall, I.M. Mishra, Adsorption of toxic metal ions onto activated carbon: Study of sorption behaviour through characterization and kinetics, *Chem. Eng. Process. Process Intensif.* 47(8) (2008) 1269–1280.
- [6] E. Erdem, N. Karapinar, R. Donat, The removal of heavy metal cations by natural zeolites, *J. Colloid Interface Sci.* 280(2) (2004) 309–314.

- [7] T.S. Jamil, H.S. Ibrahim, I.H.A. Maksoud, S.T. El-Wakeel, Application of zeolite prepared from Egyptian kaolin for removal of heavy metals. I. Optimum conditions, *Desalination* 258(1) (2010) 34–40.
- [8] M.A. Shavandi, Z. Haddadian, M.H.S. Ismail, N. Abdullah, Z.Z. Abidin, Removal of Fe(III), Mn(II) and Zn(II) from palm oil mill effluent (POME) by natural zeolite, *J. Taiwan Inst. Chem. Eng.* 43(5) (2012) 750–759.
- [9] A. Sdiri, T. Higashi, T. Hatta, F. Jamoussi, N. Tase, Evaluating the adsorptive capacity of montmorillonitic and calcareous clays on the removal of several heavy metals in aqueous systems, *Chem. Eng. J.* 172(1) (2011) 37–46.
- [10] M. Eloussaief, N. Kallel, A. Yaacoubi, M. Benzina, Mineralogical identification, spectroscopic characterization, and potential environmental use of natural clay materials on chromate removal from aqueous solutions, *Chem. Eng. J.* 168(8) (2011) 1024–1031.
- [11] Y. Bulut, Z. Tez, Removal of heavy metals from aqueous solution by sawdust adsorption, *J. Environ. Sci. (China)* 19(2) (2007) 160–166.
- [12] S. Al-Asheh, F. Banat, R. Al-Omari, Z. Duvnjak, Predictions of binary sorption isotherms for the sorption of heavy metals by pine bark using single isotherm data, *Chemosphere* 41(5) (2000) 659–665.
- [13] S.S. Ahluwalia, D. Goyal, Microbial and plant derived biomass for removal of heavy metals from wastewater, *Bioresour. Technol.* 98(12) (2007) 2243–2257.
- [14] N.G. Kandile, A.S. Nasr, Environment friendly modified chitosan hydrogels as a matrix for adsorption of metal ions, synthesis and characterization, *Carbohydr. Polym.* 78(4) (2009) 753–759.
- [15] G. Yuvaraja, K. Pattabhi Ramaiah, M. Veera Narayana Reddy, A. Krishnaiah, Removal of Pb(II) from aqueous solutions by *Caesalpinia Bonducella* leaf powder (cblp), *Indian J. Adv. Chem. Sci.* 1(3) (2013) 152–156.
- [16] T.J. Sudha vani, N. Sivagangi Reddy, K. Madhusudana Rao, K.S.V. Krishna Rao, R. Jayshree, A.V.R. Reddy, Development of thiourea-formaldehyde cross-linked chitosan membrane networks for separation of Cu(II) and Ni(II) ions, *Bull. Korean Chem. Soc.* 34(5) (2013) 1513–1520.
- [17] T.J. Sudha vani, N. Sivagangi Reddy, P. Ramasubba Reddy, K.S.V. Krishna Rao, R. Jayshree, A.V.R. Reddy, Synthesis, characterization, and metal uptake capacity of a new polyaniline and poly(acrylic acid) grafted sodium alginate/gelatin adsorbent, *Desalin. Water Treat.* 52(1–3) (2014) 526–535.
- [18] N. Li, B. Renbi, Copper adsorption on chitosan-cellulose hydrogel beads: Behaviors and mechanisms, *Sep. Purif. Technol.* 42(3) (2005) 237–247.
- [19] K.E. Geckeler, Polymer-metal complexes for environmental protection. Chemo remediation in the aqueous homogeneous phase, *Pure Appl. Chem.* 73(1) (2001) 129–136.
- [20] M.A. Sharaf, H.A. Arida, S.A. Sayed, A.A. Younis, A.B. Farag, Separation and preconcentration of some heavy-metal ions using new chelating polymeric hydrogels, *J. Appl. Polym. Sci.* 133(2) (2009) 1335–1344.
- [21] Ö. Ozgur, E. Sema, B. Yakup, K. Senol, A. Nahit, S. Nurettin, Utilization of magnetic hydrogels in the separation of toxic metal ions from aqueous environments, *Desalination* 260(1–3) (2010) 57–64.
- [22] A.T. Paulino, L.A. Belfiore, L.T. Kubota, E.C. Muniz, E.B. Tambourgi, Efficiency of hydrogels based on natural polysaccharides in the removal of Cd<sup>2+</sup> ions from aqueous solutions, *Chem. Eng. J.* 168(1) (2011) 68–76.
- [23] X.W. Peng, L.X. Zhong, J.L. Ren, R.C. Sun, Highly effective adsorption of heavy metal ions from aqueous solutions by macroporous xylan-rich hemicelluloses-based hydrogel, *J. Agric. Food. Chem.* 60(15) (2012) 3909–3916.
- [24] W.S. Wan Ngah, C.S. Endud, R. Mayanar, Removal of copper(II) ions from aqueous solution onto chitosan and cross-linked chitosan beads, *React. Funct. Polym.* 50(2) (2002) 181–190.
- [25] W.S. Wan Ngah, A. Kamari, Y.J. Koay, Equilibrium and kinetics studies of adsorption of copper(II) on chitosan and chitosan/PVA beads, *Int. J. Biol. Macromol.* 34(1) (2004) 155–161.
- [26] S. Liang, G. Xue-yi, F. Ning-chuan, T. Qing-hua, Effective removal of heavy metals from aqueous solutions by orange peel xanthate, *Trans. Nonferrous Met. Soc. China* 20 (2010) s187–s191.
- [27] A.A.A. Emara, M.A. Tawab, M.A. El-ghamry, M.Z. Elsabbe, Metal uptake by chitosan derivatives and structure studies of the polymer metal complexes, *Carbohydr. Polym.* 83(1) (2011) 192–202.
- [28] M. Monier, D.M. Ayad, D.A. Abdel-Latif, Adsorption of Cu(II), Cd(II) and Ni(II) ions by cross-linked magnetic chitosan-2-aminopyridine glyoxal Schiff's base, *Colloids Surf. B* 94 (2012) 250–258.
- [29] J.L. Gong, X.Y. Wang, G.M. Zeng, L. Chen, J.H. Deng, X.R. Zhang, Q.Y. Niu, Copper (II) removal by pectin-iron oxide magnetic nanocomposite adsorbent, *Chem. Eng. J.* 185–186 (2012) 100–107.
- [30] C. Rolin, Commercial pectin preparations, in: G.B. Seymour, J.P. Knox (Eds.), *Pectins and their Manipulation*, Blackwell Publishing, Oxford, 2002, pp. 222–241.
- [31] M. Ihl, G. Astete, V. Bifani, Precipitation of pectins from apple pomace from the Araucania region of Chile with ethanol or aluminium chloride, *Rev. Espanola. Cien. Technol. Aliment.* 32 (1992) 185–197.
- [32] K. Osamu, F. Takayuki, Y. Eiji, Characterization of the pectin extracted from citrus peel in the presence of citric acid, *Carbohydr. Polym.* 74(3) (2008) 725–730.
- [33] H. Ueno, M. Tanaka, M. Hosino, M. Sasaki, M. Goto, Extraction of valuable compounds from the flavedo of Citrus junos using subcritical water, *Sep. Purif. Technol.* 62(3) (2008) 513–516.
- [34] G.T. Grant, E.R. Morris, D.A. Rees, P.J.C. Smith, D. Thom, Biological interactions between polysaccharides and divalent cations: The egg-box model, *FEBS Lett.* 32 (1973) 195–198.
- [35] I. Braccini, S. Perez, Molecular basis of Ca<sup>2+</sup> induced gelation in alginates and pectins: The egg-box model revisited, *Biomacromolecules* 2(4) (2001) 1089–1096.
- [36] K.S.V. Krishna Rao, K. Madhusudana Rao, P.V. Nagendra Kumar, I.D. Chung, Novel chitosan-based pH sensitive micro-networks for the controlled release of 5-fluorouracil, *Iran. Polym. J.* 19(4) (2010) 265–276.
- [37] M. Pulat, D. Asil, Fluconazole release through semi-interpenetrating polymer network hydrogels based on chitosan, acrylic acid, and citraconic acid, *J. Appl. Polym. Sci.* 113(4) (2009) 2613–2619.
- [38] U. Yildiz, O.F. Kemik, B. Hazer, The removal of heavy metal ions from aqueous solutions by novel pH-sensitive hydrogels, *J. Hazard. Mater.* 183(1–3) (2010) 521–532.

- [39] D. Leroy, L. Maritnot, C. Jerome, R. Jerome, Determination of the stability constants of uranyl/polymer complexes by differential pulse polarography, *Polymer* 42(10) (2001) 4589–4596.
- [40] B.L. Rivas, B. Quilodran, E. Quiroz, Metal ion retention properties of water-insoluble polymers containing carboxylic acid groups, *J. Appl. Polym. Sci.* 99(3) (2006) 697–705.
- [41] R.M. Silverstein, G.C. Bassler, T.C. Morrill, *Spectrometric Identification of Organic Compounds*, Wiley, New York, NY, 1991.
- [42] A.A. Christy, Y. Ozaki, G. Gregoriou, Modern fourier transform infrared spectroscopy, in: D. Barceló (Ed.), *Comprehensive Analytical Chemistry D*, Elsevier, Amsterdam, 2001, pp. 246–254.
- [43] G.R. Mahdavinia, A. Pourjavadi, H. Hosseinzadeh, M. Zohuriaan, Modified chitosan superabsorbent hydrogels from poly(acrylic acid-co-acrylamide) grafted chitosan with salt- and pH-responsiveness properties, *Eur. Polym. J.* 40(7) (2004) 1399–1407.
- [44] M. Pulat, H. Eksi, Determination of swelling behavior and morphological properties of poly(acrylamide-co-itaconic acid) and poly(acrylic acid-co-itaconic acid) copolymeric hydrogels, *J. Appl. Polym. Sci.* 102(6) (2006) 5994–5999.
- [45] X.S. Ping, T. Yen-Peng, J.P. Chen, H. Liang, Sorption of lead, copper, cadmium, zinc, and nickel by marine algal biomass: Characterization of biosorptive capacity and investigation of mechanisms, *J. Colloid Interface Sci.* 275(1) (2004) 131–141.
- [46] M. Emine, N. Yasar, Investigations of nickel(II) removal from aqueous solutions using tea factory waste, *J. Hazard. Mater.* 127(1–3) (2005) 120–126.
- [47] H.L. Toor, Solution of the linearized equations of multicomponent mass transfer: II. Matrix methods, *AIChE J.* 10(4) (1964) 460–465.
- [48] I. Langmuir, The constitution and fundamental properties of solids and liquids. Part I. Solids, *J. Am. Chem. Soc.* 38(11) (1916) 2221–2295.
- [49] H.M.F. Freundlich, Over the adsorption in solution, *J. Phys. Chem.* 57 (1906) 385–471.
- [50] M.I. Tempkin, V. Pyzhev, Kinetics of ammonia synthesis on promoted iron catalyst, *Acta Phys. Chim. USSR* 123 (1940) 27–356.
- [51] C. Aharoni, M. Ungarish, Kinetics of activated chemisorption. II. Theoretical models, *J. Chem. Soc., Faraday Trans.* 73 (1977) 456–464.
- [52] A. Bhavna Shah, V. Ajay Shah, R. Rajesh Singh, B. Nayan Patel, Reduction of Cr(VI) in electroplating wastewater and investigation on the sorptive removal by WBAP, *Environ. Prog. Sustain. Energy* 30(1) (2011) 59–69.
- [53] T.S. Anirudhan, P.G. Radhakrishnan, Thermodynamics and kinetics of adsorption of Cu(II) from aqueous solutions onto a new cation exchanger derived from tamarind fruit shell, *J. Chem. Thermodyn.* 40(4) (2008) 702–709.
- [54] K.L. Nikolaos, Z.K. George, A.V. Alexandros, N.B. Dimitrios, Chitosan derivatives as biosorbents for basic dyes, *Langmuir* 23(14) (2007) 7634–7643.